SECED 2015 Conference: Earthquake Risk and Engineering towards a Resilient World
9-10 July 2015, Cambridge UK

COMPARISON OF EXPERIMENTAL RESULTS AND NUMERICAL MODELLING OF UNREINFORCED LOAD-BEARING MASONRY STRUCTURES SUBJECTED TO EARTHQUAKE LOADING

Christophe MORDANT[1] Vincent DENOËL[2] and Hervé DEGÉE[3]

Abstract: This paper presents a comparison of experimental tests results on unreinforced load-bearing masonry structures subjected to earthquake loading with numerical predictions. First, simple walls are submitted to cyclic and shaking table tests. Some of them include soundproofing devices in order to investigate their influence on the general behaviour in static and dynamic conditions. Additional walls with an opening and T-shaped walls are then tested under cyclic loading. The study is focused on the frame effect, the contribution of the perpendicular wall to the global strength and the efficiency of the connection. These aspects are also studied through shaking table tests on two masonry frames with T- or L-shaped piers. The main information is expressed in terms of force-displacement curves, mechanical properties and energy dissipation for the cyclic tests. The shaking table tests provide results in terms of dynamic and mechanical properties. Comparison of the results with numerical predictions is finally performed thanks to the software TREMURI.

Introduction

Unreinforced masonry is one of the most common and widespread way to build private dwellings in North-Western Europe and in Belgium in particular. Since the 1973 energy crisis, the demand in terms of building physics performances has progressively increased until the creation of "passive houses" concept at the end of the last century (International Passive House Association, n.d.), leading to the raising of new structural challenges and to the necessary development of technical solutions. In Belgium, these requirements have led to the transition from a monolithic masonry wall to the configuration illustrated in Figure 1a. The load-bearing wall (right) has now a reduced thickness and is separated from the façade (left) by a gap where thermal insulation is placed (in yellow). Over the past few years, the increasing demand for thermal performances has resulted in using highly insulating units at the bottom of the walls (e.g. one layer of AAC blocks or foamglass, see Figure 1b left and middle).

(a) (b)

Figure 1. (a) Configuration of a masonry wall in Belgium ; (b) Thermal cut with AAC blocks (left) or foamglass (middle) and acoustic cut with rubber (left)

Besides the thermal aspects, unreinforced masonry is now widely used as load-bearing system for apartment buildings up to 5 or 6 levels (Figure 2). This new application has two main consequences. On the one hand, it is necessary to ensure the individual comfort, especially the acoustic insulation requires the implementation of specific detailing, as for instance rubber layers located at the bottom and top of walls to cut the propagation of

[1] PhD student (F.R.I.A), University of Liège, Liège (Belgium), cmordant@ulg.ac.be
[2] Professor, University of Liège, Liège (Belgium), v.denoel@ulg.ac.be
[3] Professor, University of Hasselt, Hasselt (Belgium), herve.degee@uhasselt.be

acoustic vibrations (Figure 1b right). On the other hand, the increasing height and mass of the buildings increase the compressive stresses due to gravity loading, becoming closer to the strength limit.

Figure 2. Unreinforced load-bearing clay masonry used for multi-storey buildings

Although solutions have been developed to face these new structural challenges, they have to be validated for the design of unreinforced masonry structures submitted to normal and dynamic actions. Indeed, the application of the Eurocode 8 rules has become mandatory since 2011 in the European Union. These rules have been identified as rather conservative for masonry in low-to-moderate seismic regions (Karantoni and Lirantzaki, 2009) and not compatible with the common constructional habits in some countries, among which Belgium (Degée et al., 2007). Therefore, the consideration of the seismic action in the normative procedure needs being updated. This is particularly necessary since the seismic risk has become significantly higher due to the reduced wall thickness and to the increasing height and mass of buildings. Moreover, the presence of specific detailing at the wall extremities for acoustic and thermal reasons also influences the structural stability as it results in a disconnection between walls and floors, which goes in a way opposite to the basic principle of the seismic resistance ("box-type" behaviour). Nevertheless, these details are not considered in the current seismic codes.

In the perspective of updating the existing design procedures and of validating new specific detailing, cycling loading tests have been performed at the University of Liège and shaking table tests have been carried out in the framework of the SERIES project at the University of Bristol. These experimental campaigns first study the behaviour of simple unreinforced load-bearing clay masonry walls in static and dynamic conditions. Then, walls with soundproofing rubber devices are tested with the aim of investigating their influence on the static and dynamic behaviour of walls. Finally, simple walls with an opening and T-shaped walls with different compression ratio are submitted to cyclic loading, while shaking table tests are performed on unreinforced masonry frames with T- or L-shaped piers. These specimens are tested in order to study the frame effects and/or the contribution of perpendicular walls in the global strength given that these latter are not considered yet. Former experimental tests have been performed (da Porto et al., 2010; Costa et al., 2011; Beyer and Mangalathu, 2013; Sousa et al., 2014). They are however focused on different masonry types and only a few are interested in new specific detailing (Martens, 2014).

First the experimental results of the cyclic loading tests are given. The main outcomes are expressed in terms of crack pattern, force-displacement curve, energy dissipation and mechanical properties. Then, the exploitation of the shaking table tests are briefly summarized. Details of this campaign are given in (Mordant et al., 2014; Mordant et al., 2015a). Comparisons evidence the influence of the wall length and of the presence of the rubber layers on the structural behaviour. This latter also depends on the frame effect and the experimental results outline the importance of a proper consideration for the perpendicular walls in the assessment procedures. Differences between (static) cyclic and shaking table tests are also highlighted. Dynamic phenomena like rocking can indeed not be observed during static cyclic tests. Finally, the tested specimens are modelled with the software TREMURI (Lagomarsino et al., 2013) in order to compare the experimental results with the model predictions in terms of general behaviour, failure modes and force-displacement curves. The comparisons are expected to validate the numerical model and to provide information for its improvement, especially regarding the connection between perpendicular walls.

Cyclic loading tests

Cyclic loading tests are performed on thin-bed layered unreinforced load-bearing masonry walls with glued horizontal joints and empty vertical ones. The geometry of the specimens and the mechanical properties of the masonry units are tabulated in Table 1 and Table 2 respectively. There are five simple walls among which one includes rubber layers at its bottom and top (A2) and three others have an opening created by a lintel with different support lengths (A3-5). These latter are all unsymmetrical and one of them is reinforced with "Murfor" (Bekaert, n.d.) placed every second horizontal mortar layer (A5). Three T-shaped walls built in the same way, but with different units are also tested. These walls are submitted to different compression level (0.75/1.00/1.25 MPa) and are made of two walls, the main one is called "shear wall" while the second is dubbed the "flange". These walls are vertically glued together. Figure 3 illustrates a wall with an opening (left) and a T-shaped wall (right). All walls are built between two RC beams modeling rigid floors and are instrumented with force and displacements sensors.

Table 1. Geometry of the cycling load tested specimens

Specimen	A 1	A 2	A 3	A 4	A 5	C 1	C 2	C 3
Length [mm]	3000	3000	3000	3000	3000	2650	2650	2650
Height [mm]	2800	2800	2800	2800	2800	2800	2800	2800
Thickness [mm]	139.6	139.6	139.6	139.6	139.6	150.0	150.0	150.0
Compression stress [MPa]	1.00	0.50	1.00	1.00	1.00	0.75	1.00	1.25
Length opening [mm]	/	/	900	900	900	/	/	/
Height opening [mm]	/	/	2000	2000	2000	/	/	/
Length support [mm]	/	/	150	450	150	/	/	/
Length flange [mm]	/	/	/	/	/	1500	1500	1500
Height flange [mm]	/	/	/	/	/	2800	2800	2800

Table 2. Masonry mechanical properties of the cycling load tested specimens

Specimen		A 1-5	C 1-3
Normalized compressive strength of units (EN 772-1 Annex A)	[MPa]	13	15
Measured characteristic masonry compressive strength (EN 1052-1)	[MPa]	5.6	6.5
Characteristic compressive strength (EN 1996-1-1)	[MPa]	4.2	/
Characteristic compressive strength (NBN-EN 1996-1-1)	[MPa]	3.9	5
Initial shear strength (NBN-EN 1996-1-1)	[MPa]	0.3	0.3
Maximum characteristic shear strength (NBN-EN 1996-1-1)	[MPa]	0.585	0.675

Figure 3. Illustration of (left) a simple wall with an opening (A 3/A 5) and (right) a T-shaped wall (C 1-3)

Details of the instrumentation layout are given in Figure 4 (left) for the simple walls. Relative displacement sensors are only placed when rubber devices are present to capture their influence. Another layout has been chosen for T-shaped walls considering the different geometry and objectives (see Figure 4, right). According to the testing procedure, the vertical load is first introduced through two pairs of "Dywidag" bars. As given in Table 1, the imposed compression level is 1 MPa for simple walls without rubber devices and 0.5 MPa for the wall with rubber devices. The stress level in the T-shaped walls varies from 0.75 to 1.25 MPa. The horizontal loading is then applied to the upper RC beam by the application of a cyclic imposed horizontal displacement with an increment, depending on the specimen response.

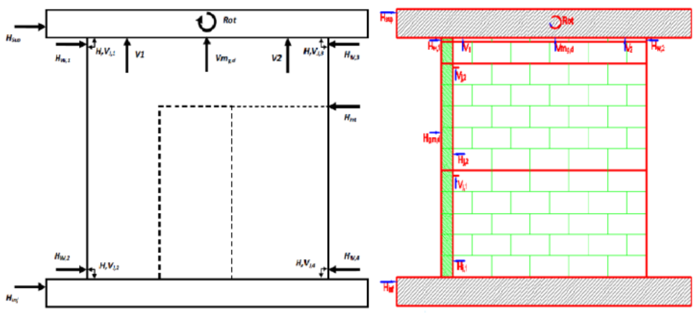

H_{Sup}	Global horizontal displacement of the upper RC beam
H_{Inf}	Global horizontal displacement of the lower RC beam
$H_{g,m,d}$	Global horizontal displacement of the secondary wall(left, middle and right)
V_1 V_2	Global vertical displacement measured at the bottom face of the upper RC beam
Vm_g Vm_d	Global vertical displacement of the middle of upper RC beam measured on both sides of the wall
$H_{W,1\text{-}4}$	Global horizontal displacement of the wall measured at its edges
$H,V_{j,1\text{-}4}$	Relative displacement (vertical and horizontal) of the wall with respect to RC beam / of the secondary wall with respect to main wall
Rot	Rotation of the upper RC beam

Figure 4. Instrumentation layouts of the specimens

Direct observations of the specimens give indications about the failure mode. The specimen without any specific detailing, opening nor perpendicular wall (A1) presents classical diagonal cracks, translating a shear collapse as shown in Figure 5 (a). Concerning specimen A2, the presence of soundproofing devices is clearly highlighted by the cracking pattern. Indeed, a vertical crack starts in the upper third of the wall and is followed by diagonal cracking extending to the bottom edges, as displayed in Figure 5 (b). The vertical crack has been initiated in the compression stage and is supposedly due to the Poisson effect as the transverse tension stresses due to compression is more important in presence of a rubber layer than for the masonry. Figure 5 (c – e) illustrates the failure modes of the walls with an opening. The specimen A3 including a lintel with 0.15 m support length prematurely failed because of the local crushing of the block directly supporting the lintel (Figure 5 (c)). This unexpected collapse is no more observed when the support length of the lintel becomes longer. Indeed, specimen A4 with support length of 0.45 m exhibits diagonal cracks starting from the lintel (Figure 5 (d)). The ductility of walls with opening can be improved thanks to the solution “Murfor”. In this case, the unit below the lintel also fails, but the wall remains stable and the collapse occurs by internal crushing of the units located at mid-height (see Figure 5 (e)). Figure 6 depicts the cracks on T-shaped walls. The crack repartition is similar for all three compression levels and concerns the shear wall. No damages were observed at the connection between the shear wall and the flange, leading to the conclusion that a vertical glued joint is fully efficienct in this testing configuration.

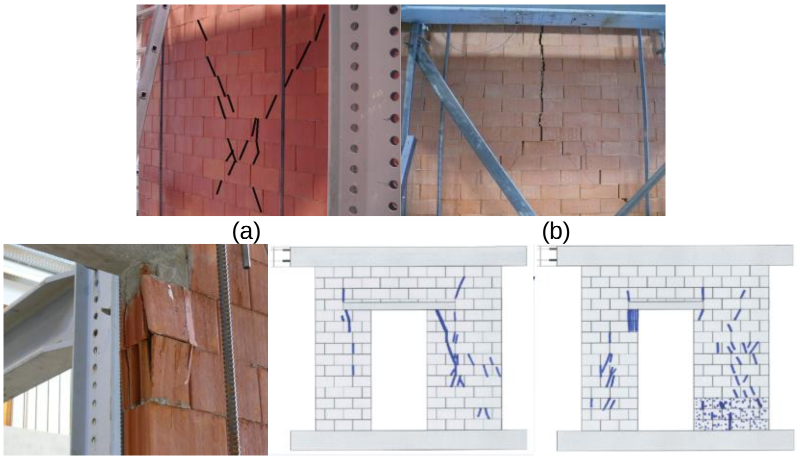

(a) (b)

(c) (d) (e)

Figure 5. Crack patterns of the simple walls with/out rubber layers or an opening

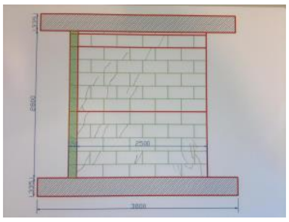

Figure 5. Crack patterns of the T-shaped walls

The main specific result of cyclic loading tests is the force-displacement curve. From this curve, it is possible to determine the envelope and to convert it to an equivalent bilinear elastic-perfectly-plastic curve defined by its initial slope and its yield strength using a least-square fitting. This procedure is performed for each specimen. An example is given in Figure 7 for the simple walls without and with rubber devices.

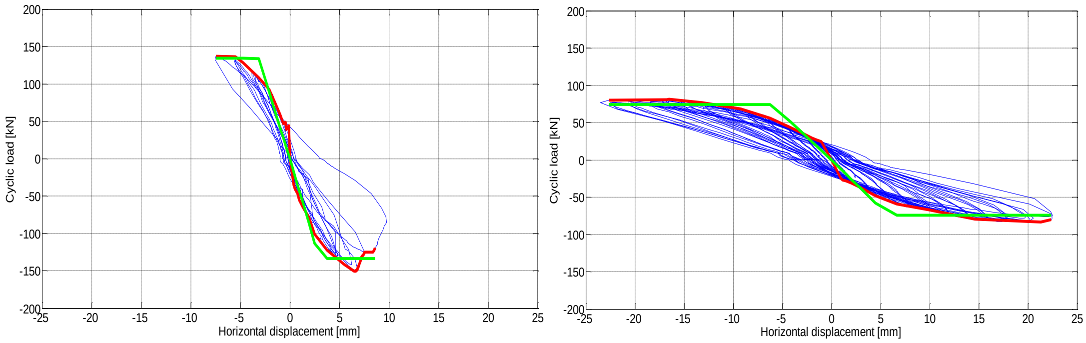

(a) (b)

Figure 7. Force-displacement curve of the simple walls without (a) and with (b) rubber devices

In Figure 7, the raw data is represented in blue and the red curve is the envelope. The influence of the acoustic devices is easily observable and involves higher horizontal displacements with a lower load, as expected in the view of the higher deformability of the rubber layers. The bilinear curve (in green) provides information about the ultimate loads and drifts and the ductility, see also Table 3.

Table 3. Information obtained from the force-displacement curve

Specimen	A 1	A 2	A 3	A 4	A 5	C 1	C 2	C 3
Ultimate load + [kN]	133.0	73.8	76.1	82.0	76.9	104.4	138.8	161.7
Ultimate load + [kN]	137.1	74.3	73.8	76.6	71.2	125.6	158.1	172.5
Ultimate drift + [mm]	7.5	23.5	8.8	5.3	7.2	6.71	5.22	4.91
[%]	0.27	0.84	0.30	0.19	0.26	0.24	0.19	0.17
Ultimate drift - [mm]	8.4	22.2	7.4	6.1	8.0	7.71	4.88	5.33
[%]	0.30	0.79	0.26	0.22	0.29	0.27	0.17	0.19
Ductility + [-]	1.8	3.1	1.7	1.7	2.3	3.43	1.99	1.84
Ductility - [-]	1.7	2.9	1.1	1.8	2.6	3.06	2.43	2.27
Energy dissipation [Nm]	2517	15 759	1149	1288	3377	7676	4807	4029

The data given in Table 3 first provides information about the ultimate load. The simple wall A1 is chosen as reference. The presence of rubber (specimen A2) or of an opening (specimens A3-5) significantly reduces the maximum sustainable load, up to 48%. On the contrary, if the influence of the wall length is neglected, connecting the shear wall to a perpendicular wall slightly increases the resistance (+4% to +15%), the compression level being the same (specimen C2). The ultimate load increase obviously becomes more important with the increase of the compression level (specimen C3). Then, the behaviour of the specimens can also be compared based on the ultimate drift and the correlated ductility. Concerning the influence of the rubber, the values in Table 3 confirm the comments on the Figure 7. Indeed, the ultimate drift is around three times larger in presence of these soundproofing devices. The perpendicular wall has an opposite effect and leads to a reduced drift, corresponding to stiffer specimens as expected. In terms of ductility, the acoustic layers and the perpendicular wall have both positive repercussions. Regarding the walls with an opening, differences appear. The ductility is lower for the specimen which has a lintel with short support length due to the crush of the units below the lintel. Lengthening the support length restores the ductility of the simple wall, while using the “Murfor” system enhances it substantially. Concerning the T-shaped walls, the increase of the compression level involves a smaller ductility, the presence of the flange having however advantages especially in one direction. Finally, Table 3 compares the specimens behaviour thanks to the energy dissipated during the cyclic test. Once again, the soundproofing elements enhance the behaviour as the energy dissipation is multiplied by six in comparison to the reference wall. This positive influence is also observed to a lesser extent when there is a perpendicular wall. In the case of walls with an opening, Table 3 shows a reduction, except for the specimen with “Murfor”. To conclude the comparison, Table 3 highlights the positive effects of rubber devices and perpendicular walls on the behaviour of simple unreinforced masonry walls. Nevertheless, these effects are questionable given that they are derived from tests on single elements and should be replaced in the context of a complete building. In particular, the rubber devices could be a problem due to the involved higher displacements and attention should be paid to the connection of T-shaped walls in other test configurations. Tests on walls with opening point out the importance of the support length of the lintel. The “Murfor” system is a possible solution to improve the wall behaviour, but is outside of the scope of unreinforced masonry.

Another and last interesting result is the assessment of the mechanical properties in order to use them in numerical models. The elastic modulus can be evaluated with the measurements taken during the compression phase, while the shear modulus is deduced from the cyclic loading phase, based on the assumption of a cantilever beam-like behaviour. Figure 8 illustrates the results of these assessments. Note that the deduced values given in Table 4 are only valid for the first horizontal loading cycles. Then, damages occur in the specimens and result in a decrease of the mechanical properties.

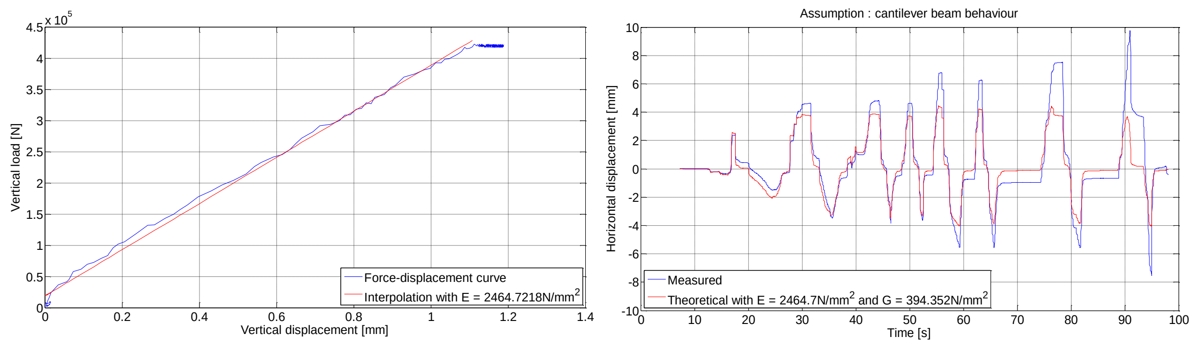

Figure 8. Assessment of the elastic (left) and shear (right) moduli

Table 4. Mechanical properties of the specimens

Specimen	A 1	A 2	A 3	A 4	A 5	C 1	C 2	C 3
Elastic modulus [MPa]	2464.7	2464.7	2425.9	3542.5	3864.6	2773.6	3692.8	3662.5
Shear modulus [MPa]	394.4	394.4	218.3	351.9	314.4	346.7	477.4	561.4

Shaking table tests

Four simple unreinforced masonry walls with thin-bed layered horizontal joints and empty vertical ones, were tested on the shaking table at the EQUALS laboratory. The walls have two different lengths, namely 0.72 m and 2.10 m, and one wall of each length includes acoustic devices. An additional 5 tons mass has been placed on the wall top to simulate structural load (Figure 9). The mason-work and masonry units are the same than the ones used for the simple walls tested in Liège. The walls have been shaken with increasing acceleration input and their modal properties identified before each seismic test.

Figure 9. Specimens tested on the shaking table

The results of this experimental campaign have been extensively exploited in previous contributions and it was observed a significant rocking behaviour for the higher acceleration input, strongly dependent on the wall length and the presence of soundproofing devices. These tests have led to the elaboration of a frequency equation corresponding to the specific configuration of the current tests in order to obtain the mechanical properties of the tested walls (Mordant et al., 2015b). Another outcome is the development of a rocking model taking into account the presence of rubber layers (Mordant et al., 2015c).

In the perspective of modelling these walls in TREMURI software, only the useful results are given in the following, namely the results of a preliminary assessment design according to Eurocode 8 (EN 1998-1-1:2004), the measured fundamental frequency and the mechanical properties. This information is tabulated in Table 5 and Table 6. The fundamental frequency and mechanical properties only concern the walls without rubber layers because the modelling of these specific detailing is not possible actually.

Table 5. Preliminary assessment design of walls without rubber

Specimen	Compression level [MPa]	Maximum horizontal load [N]	Acceleration [m/s²]
0.72 m long specimen	0.5	9000	0.7
2.10 m long specimen	0.2	26200	2.0

During the experimental phase, the walls have been submitted to acceleration three times higher than the ones obtained by the design. At this stage, the walls did not collapse because of the rocking behaviour.

Table 6. Fundamental frequency and mechanical properties of the walls without rubber

Specimen	Fundamental frequency [Hz]	Elastic modulus [N/mm²]	Shear modulus [N/mm²]
0.72 m long specimen	4.04	2515	1006
2.10 m long specimen	9.43	2515	153.4

The experimental tests on masonry frames with T- or L-shaped piers are not detailed here because their modelling in the numerical tool require more time.

Comparison with numerical predictions

This section is dedicated to the comparison of experimental results presented here above with numerical predictions given by TREMURI. In this program, the structures are modelled using nonlinear macro-elements and a nonlinear pushover analysis is performed based on seismic analysis approaches adopted by different codes, among which Eurocode 8. It is also possible to perform a modal analysis.

On the one hand, the comparison is made for the specimens tested on the shaking table. Model inputs are the wall geometry, the load and the mechanical characteristics. As the natural frequencies of the walls has been assessed thanks to white noise tests, a first comparison point is the fundamental frequencies. These ones are given in Table 7. The second point of comparison cannot be the maximum sustainable load or the related horizontal displacement given that the theoretically predicted failure mode based on a pushover analysis is a shear failure, while a global dynamic rocking behaviour has actually been observed in both situations. The results of the pushover analysis performed by the model can be however compared to the preliminary assessment design, as it is in Table 8.

Table 7. Comparison of the fundamental frequency

Specimen	Experimental [Hz]	Numerical [Hz]
0.72 m long specimen	4.04	4.58
2.10 m long specimen	9.43	9.04

Table 8. Comparison of the maximum horizontal load

Specimen	Preliminary assessment [N]	Numerical [Hz]
0.72 m long specimen	9000	8950
2.10 m long specimen	26200	25840

Table 7 shows differences between experimental measurements and numerical predictions in terms of natural frequencies. These differences are expected as the additional mass used to load the walls is represented by a linear distributed load in the program. Thus, two main parameters are not considered in the modelling, namely the rotary inertia and the distance between the wall top and the mass centroid. The influence of these parameters has been studied in (Mordant et al., 2015b). Correction factors of 0.86 for the 0.72 m long wall and of 1.03 for the 2.10 m long wall have been found in this previous work and have to be applied to the values obtained by the model, leading to natural frequency of 3.94 Hz and 9.34 Hz respectively. The corresponding relative error is then 2.45% and 0.95%. In Table 8, the preliminary assessment and the numerical predictions are in good agreements. On the other hand, results of the numerical modelling for cyclic tested specimens are tabulated in Table 9. Specimens A2 and A4 are not included because the rubber layers cannot be modelled, while the "Murfor" system acts like reinforcements which is out of the scope of the present research.

Table 9. Information obtained from the force-displacement curve

	Ultimate load + [kN]		Ultimate load - [kN]		Ultimate drift + [mm]		Ultimate drift - [mm]		Ductility + [-]		Ductility - [-]	
	Exp.	Num.	Exp.	Num.	Exp.	Num.	Exp.	Num.	Exp.	Num.	Exp.	Num.
A1	133.0	143.5	137.1	145.4	7.5	10.6	8.4	10.6	1.8	2.7	1.7	2.7
A3	76.1	47.0	73.8	44.9	8.8	19.6	7.4	9.6	1.7	3.2	1.1	1.7
A4	82.0	46.0	76.6	45.3	5.3	10.6	6.1	11.6	1.7	3.0	1.8	3.5
C1	104.4	105.9	125.6	117.6	6.71	10.7	7.71	11.5	3.4	5.37	3.1	5.19
C2	138.8	134.1	158.1	142.3	5.22	10.7	4.88	11.5	2.0	6.1	2.4	6.27
C3	161.7	149.38	172.5	172.31	4.91	10.7	5.33	11.5	1.8	6.27	2.3	5.86

The analysis of Table 9 for the reference wall A1 highlights a rather good prediction of the ultimate load. The relative error between experimental and numerical values is around 7.8% at most. On the contrary, the assessment of the ultimate drift provides values quite different from those obtained with the equivalent bilinear curve (from 26 to 41%). This difference also impacts the ductility as it is defined as the ratio between the ultimate displacement and the displacement corresponding to the yield limit. These observations are also valid for the modelling of T-shaped walls (C1-3). In this case, a rigid connection between perpendicular walls has been assumed and is in accordance with the experimental reality. The disagreement in terms of ultimate displacement possibly comes from the definition of a maximum theoretical value depending on the failure mechanisms. In the present case, a shear failure is observed and the ultimate displacement is equal to 0.4% of the wall height. Such a value could be irrelevant for the studied type of masonry. Regarding specimens with an opening, major differences are observed as well in terms of ultimate load as in terms of ultimate displacement. Additional investigations are required to enhance the numerical results. Main issues are the modelling of the spandrel behaviour (horizontal element of the equivalent frame) and the height of the masonry piers. This latter can indeed vary, as shown in Figure 10, as the modelling by an equivalent frame consists in defining piers and spandrels as beam elements (in green). These elements are then linked together thanks to rigid elements (in blue) whose definition remains based on some subjective criteria.

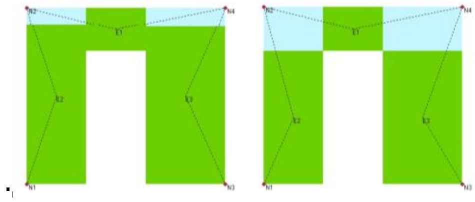

Figure 9. Different possible models of a wall with an opening

Conclusions

This paper deals with experimental tests on thin-bed layered unreinforced load-bearing clay masonry sub-structures submitted to earthquake loading and their comparison with numerical predictions obtained by the software TREMURI. A first experimental campaign consists in cycling loading tests and a second one uses shaking table tests. Both campaigns aim at studying the behaviour of unreinforced masonry walls and at investigating the influence of the presence of rubber layers placed for acoustic reasons on their dynamic and static behaviour. Additional specimens have been tested with the perspective of developing a better understanding of the behaviour of walls with an opening and of evaluating the contribution of perpendicular walls in the global strength. These campaigns lead to the following conclusions.

First, the general behaviour of simple masonry walls is relatively well captured by TREMURI when they are submitted to cyclic loading tests. Shaking table tests however lead to dynamic phenomena, like rocking. Such phenomenon cannot be considered in the software.

Then, the presence of soundproofing devices has a direct influence on the general behaviour. In static conditions, the failure mode changes and the ultimate load is significantly reduced while the horizontal displacements increase. Nevertheless, these devices allow a better energy dissipation. Although they also increase displacements in dynamic conditions, the rubber layers have positive effects. For instance, they limit the wall damage because of the capacity of the rubber to absorb the impact energy. This is translated by the transition from the rocking behaviour of a rigid block on a rigid foundation to a rigid block resting on a flexible support. Improvements of numerical models have to be done in order to be able to consider these specific detailing.

Finally, the modelling of walls with an opening and T-shaped walls leads to opposite conclusions. The modelling of the former requires additional investigations to improve the response. Two main issues have been identified, namely the height of the masonry piers and the behaviour of spandrel elements. The latter have shown interesting results, especially in terms of ultimate load. A particular attention should however be paid to the connection between perpendicular walls, for which numerical predictions in terms of displacements show significant discrepancies.

Acknowledgments

The research leading to these results has received funding from the European Union Seventh Framework Programme (FP7/2007-2013) under grant agreement n° 227887, SERIES. C. Mordant also acknowledges the F.R.S - FNRS (Belgian fund for research) for the support of his PhD and Davide Seni (S.T.A. DATA S.r.l.) for the technical support.

REFERENCES

Bekaert (n.d.), Murfor ® masonry reinforcement, Retrieved February 10, 2015, from http://www.bekaert.com/en/products/construction/masonry-reinforcement

Beyer K and Mangalathu S (2013) Review of strength models for masonry spandrels. *Bulletin of Earthquake Engineering,* 11:512-542

Costa AA, Penna A & Magenes G (2011) Seismic performance of Autoclaved Aerated Concrete (AAC) Masonry: From Experimental Testing of the In-Plane Capacity of Walls to Building Response Simulation. *Journal of Earthquake Engineering*, 15: 1-31

da Porto F, Guidi G, Garbin E and Modena C (2010) In-Plane Behavior of Clay Masonry Walls: Experimental Testing and Finite-Element Modeling, *Journal of Structural Engineering*, 136:1379-1392

Degée H, Denoël V, Candeias P, Campos Costa A and Coelho E (2007) *Experimental investigation on the seismic behaviour of North-European masonry houses*. 7° Congresso de Sismologia e Engenharia Sismica (SISMICA), Porto, Portugal, 26-27-28 September

EN 1998-1-1: 2004: *Eurocode 8: Design of structures for earthquake resistance – Part 1: General rules, seismic actions and rules for buildings*. December 1994

International Passive House Association (n.d.) Passive House, Retrieved February 10, 2015, from www.passivehouse-international.org/index.php?page_id=78

Karantoni FV and Lirantzaki FN (2009). *Seismic behaviour of "Simple Masonry Buildings" according to EN 1998*. 7th International Conference on Earthquake Resistant Engineering Structures, Limassol, North Cypris, 11-12-13 May

Lagomarsino S, Penna A, Galasco A and Cattari S (2013) *TREMURI program: an equivalent frame model for the nonlinear seismic analysis of masonry buildings*. Engineering Structures, 56:1787-1799

Martens D (2014) *Thermal Break with Cellular Glass Units in Load-Bearing Masonry Walls*. 9th International Masonry Conference, (IMC), Guimaraes, Portugal, 7-8-9 July

Mordant C, Dietz M, Taylor C, Plumier A and Degée H (2014) *Seismic behaviour of thin-bed layered unreinforced clay masonry shear walls including soundproofing elements*, Chapter 6. In: Seismic Evaluation and Rehabilitation of Structures, eds Alper Ilki and Mochal N. Fardis, Geotechnical, Geological and Earthquake Engineering series Vol. 26, Springer International Publishing Switzerland 2014, 77-93

Mordant C, Dietz M, Taylor C and Degée H (2015a) *Seismic behaviour of thin-bed layered unreinforced clay masonry frames with T- or L-shaped piers*. In: Seismic Evaluation and Rehabilitation of Structures, eds Alper Ilki and Mochal N. Fardis, Geotechnical, Geological and Earthquake Engineering series, Springer 2015. (in press)

Mordant C, Denoël V and Degée H (2015b) *Characterization of mechanical properties of unreinforced load-bearing masonry walls including soundproofing devices thanks to the Timoshenko beam theory and based on experimental shaking table tests.* (to be submitted)

Mordant C, Degée H and Denoël V (2015c) *Rocking behaviour of simple unreinforced load-bearing masonry walls including soundproofing rubber layers*. 5th ECCOMAS Thematic Conference on Computational Methods in Structural Dynamics and Earthquake Engineering (COMPDYN 2015), Crete Island, Greece, 25-27 May 2015 (submitted)

Sousa LC, Sousa H, Castro CF, Antonio CC and Sousa R (2014) A new lightweight masonry block: Thermal and mechanical performance, *Archives of civil and mechanical engineering*, 14:160-169